Vaccinia virus cores are transported on microtubules

Gemma C. Carter,[1] Gaener Rodger,[1,2]† Brendan J. Murphy,[1] Mansun Law,[1,2] Oliver Krauss,[2]‡ Michael Hollinshead[1,2] and Geoffrey L. Smith[1,2]

[1]Department of Virology, Faculty of Medicine, Imperial College London, St Mary's Campus, Norfolk Place, London W2 1PG, UK

[2]Sir William Dunn School of Pathology, University of Oxford, South Parks Road, Oxford OX1 3RE, UK

Correspondence
Geoffrey L. Smith
(at Imperial College)
glsmith@imperial.ac.uk

Received 3 April 2003
Accepted 6 June 2003

Infection with *Vaccinia virus* (VV) produces several distinct virions called intracellular mature virus (IMV), intracellular enveloped virus (IEV), cell-associated enveloped virus (CEV) and extracellular enveloped virus (EEV). In this report, we have investigated how incoming virus cores derived from IMV are transported within the cell. To do this, recombinant VVs (vA5L-EGFP-N and vA5L-EGFP-C) were generated in which the A5L virus core protein was fused with the enhanced green fluorescent protein (EGFP) at the N or C terminus. These viruses were viable, induced formation of actin tails and had a plaque size similar to wild-type. Immunoblotting showed the A5L-EGFP fusion protein was present in IMV particles and immunoelectron microscopy showed that the fusion protein was incorporated into VV cores. IMV made by vA5L-EGFP-N were used to follow the location and movement of cores after infection of PtK_2 cells. Confocal microscopy showed that virus cores were stained with anti-core antibody only after they had entered the cell and, once intracellular, were negative for the IMV surface protein D8L. These cores co-localized with microtubules and moved in a stop–start manner with an average speed of 51·8 ($\pm$3·9) μm min^{-1}, consistent with microtubular movement. Treatment of cells with nocodazole or colchicine inhibited core movement, but addition of cytochalasin D did not. These data show that VV cores derived from IMV use microtubules for intracellular transport after entry.

INTRODUCTION

Vaccinia virus (VV) replicates in cytoplasmic factories (Moss, 2001) and produces structurally distinct forms of infectious progeny (Smith *et al.*, 2002). The first infectious virion formed is called intracellular mature virus (IMV) and this remains in the cell until cell lysis. Although IMV represents the majority of infectious progeny, it is not sufficient for efficient cell-to-cell spread and this function is performed by virions that contain an additional lipid membrane (Rodriguez & Smith, 1990; Blasco & Moss, 1991). Some IMV are transported away from factories to near the microtubule-organizing centre (MTOC) where they are wrapped by a double membrane to form intracellular enveloped virus (IEV). IEV then move to the cell periphery where they fuse with the plasma membrane to produce cell-associated enveloped virus (CEV) on the cell surface. The CEV particle induces actin polymerization beneath the plasma membrane to propel the virion away from the cell or into an adjacent cell. If a CEV particle becomes detached from the cell it is called extracellular enveloped virus (EEV). EEV mediate the long-range transmission of virus within the host. For a review of the roles of the different virions in the virus life-cycle see Smith *et al.* (2002).

The transport of a large virus such as VV with dimensions of 250 by 350 nm would be an inefficient process in the cytosol without specific transport mechanisms and it has been estimated that diffusion of VV across 10 μm of cytosol would take 5·7 h (Sodeik, 2000). Therefore, VV has evolved to exploit host cell transport machinery. IMV particles are transported on microtubules from virus factories to near the MTOC. This process requires the A27L protein, because if expression of the *A27L* gene is repressed, IMV are not transported away from factories (Sanderson *et al.*, 2000). Once IMV are wrapped to form IEV, the IEV particles are transported on microtubules to the cell surface (Geada *et al.*, 2001; Hollinshead *et al.*, 2001; Rietdorf *et al.*, 2001; Ward & Moss, 2001b). Two VV proteins have been implicated in this transport: F12L and A36R. In the absence of F12L, IEV are

†Present address: Division of Virology, IBLS, University of Glasgow, Church Street, Glasgow G11 5JR, UK.

‡Present address: Dorfstrasse 28, 64720 Michelstadt, Germany.

formed but not transported to the cell surface (Zhang *et al.*, 2000; van Eijl *et al.*, 2002). In the absence of A36R, both IEV and CEV are formed (Sanderson *et al.*, 1998; Wolffe *et al.*, 1998; van Eijl *et al.*, 2000, 2002; Hollinshead *et al.*, 2001), indicating virion transport, although it has been reported that the A36R protein affects IEV transport (Rietdorf *et al.*, 2001). However, the A36R protein is not essential for transport because viruses lacking A36R and with mutations in either the A33R or B5R proteins release enhanced levels of EEV (Katz *et al.*, 2002).

Once CEV are formed on the cell surface, actin filaments polymerize on the cytosolic face of the plasma membrane beneath CEV particles (van Eijl *et al.*, 2000; Hollinshead *et al.*, 2001; Ward & Moss, 2001b). Originally, these actin tails were proposed to form on IEV particles (Cudmore *et al.*, 1995, 1996a; Frischknecht *et al.*, 1999) but they appear only after CEV formation and their role is to drive the CEV particles into surrounding cells. The A36R protein is essential for actin tail formation (Sanderson *et al.*, 1998; Wolffe *et al.*, 1998; Frischknecht *et al.*, 1999), although mutations in other EEV proteins (A33R, A34R, F13L and B5R) also cause a reduction in actin tail formation; for a recent review see Smith *et al.* (2002). The importance of actin tail formation in cell-to-cell spread was illustrated by a side-by-side comparison of mutants lacking each EEV or IEV specific protein (Law *et al.*, 2002). In all cases where the production of actin tails was inhibited the virus had a small plaque phenotype.

The binding and entry of VV into uninfected cells have been controversial and different models have been proposed. When considering VV entry it is necessary to define which form of virus is being described. The IMV and EEV forms are both infectious, although the EEV form has a higher specific infectivity (Vanderplasschen & Smith, 1997), but these virions are surrounded by different numbers of membranes and so they face different problems during entry. The number of membranes around an IMV particle has been disputed; some authors have claimed a single membrane (Dales & Siminovitch, 1961; Morgan, 1976; Hollinshead *et al.*, 1999) whereas others have claimed at least two (Sodeik *et al.*, 1993; Griffiths *et al.*, 2001a, b; Risco *et al.*, 2002). If IMV has a single membrane then EEV has two; if IMV has two then EEV has three. Before transcription of the virus genome can commence in the cytosol all membranes surrounding the core must be shed or permeabilized. Previously, several IMV proteins were reported to be lost during virus entry (Vanderplasschen *et al.*, 1998; Pedersen *et al.*, 2000) and some cores were found to co-localize with microtubules (Mallardo *et al.*, 2001).

Virus replication occurs in factories in the perinuclear region of the cytoplasm. The transport of virus cores to this site is addressed here. Several recombinant VVs have been described in which the green fluorescent protein (GFP) or enhanced GFP (EGFP) was fused to a protein in the EEV envelope. Either the B5R (Hollinshead *et al.*, 2001; Ward & Moss, 2001a; Rodger & Smith, 2002) or F13L (Ward & Moss, 2000; Geada *et al.*, 2001; Husain & Moss, 2001; Rietdorf *et al.*, 2001) proteins have been used. These viruses have been used to follow the location and movement of individual proteins or whole virions in the cell. To investigate the movement of virus cores, it was necessary to have EGFP fused to a core protein. We selected gene *A5L* from VV strain Western Reserve (WR) for this purpose. This gene is called *A4L* in VV Copenhagen (Goebel *et al.*, 1990) and the gene product has also been called p39 (Maa & Esteban, 1987; Demkowicz *et al.*, 1992; Cudmore *et al.*, 1996b). A5L is present on the surface of the core of IMV (Cudmore *et al.*, 1996b) and of cores released into the cytosol during infection (Pedersen *et al.*, 2000). The protein is essential for the formation of infectious IMV (Williams *et al.*, 1999). Despite the requirement for A5L, we were able to replace the wild-type *A5L* gene with *A5L* fused to *EGFP* at either terminus. IMV derived from vA5L-EGFP-N was used to follow the movement of cores after infection of new cells by using time-lapse fluorescent microscopy. Data presented show that cores move inward from the cell periphery using microtubules. Thus VV uses microtubules for multiple stages of its life-cycle.

METHODS

Cells. CV-1, TK$^-$143B and RK_{13} cells were grown in minimum essential medium (MEM) supplemented with 10 % heat-inactivated foetal bovine serum (FBS) (Gibco). D98OR and BS-C-1 cells were grown in Dulbecco's modified Eagle's medium (DMEM) (Gibco) with 10 % FBS. PtK_2 cells (a gift from Louise Cramer, University College London, UK) were grown in low-glucose DMEM (Gibco) with 10 % FBS. Virus infections were performed in DMEM with 2 % FBS, except for PtK_2 cells where low glucose DMEM with 2·5 % FBS was used.

Plasmid construction. Fusion of EGFP to the N or C terminus of A5L was achieved by PCR splicing by overlap extension (Horton *et al.*, 1989) using VV strain WR genomic DNA as template. For the C-terminal fusion, oligonucleotides (1) 5′-CTCCGTTGAATTCGATGACTATAGGACAAGAACCCTCCTC-3′ and (2) 5′-CAGCTCCTCGCCCTTGCTCACCTTTTGGAATCGTTCAAAACC-3′ were used to generate a 1303 bp fragment containing the A5L ORF and 433 bp upstream. Oligonucleotides (3) 5′-GGCATGGACGAGCTGTACAAGTAATAAGATTGGATATTAAAATCACGCTTTCGAG-3′ and (4) 5′-CGTACTCCAAGCTTGTGTAGATGCTACTTCGTCGATGG were used to generate a PCR fragment 375 bp downstream of the A5L ORF. The EGFP ORF was amplified using pEGFPC1 (Clontech) as template and oligonucleotides (5) 5′-GTGAGCAAGGGCGAG-3′ and (6) 5′-CTTGTACAGCTC-3′ generating a 714 bp fragment. Oligonucleotides (1) and (4) introduced *Eco*RI and *Hin*dIII restriction sites, respectively (underlined), while oligonucleotides (2) and (3) contained EGFP sequences enabling the individual fragments to be assembled into a single 2392 bp gene. This was digested with *Eco*RI and *Hin*dIII and cloned into *Eco*RI- and *Hin*dIII-digested pSJH7 (Hughes *et al.*, 1991) to form pA5L-EGFP-C.

For the N-terminal fusion, oligonucleotides (1) and (7) 5′-CAGCTCCTCGCCCTTGCTCACCATTTAAGGCTTTAAAATTGAATTGCG-3′ were used to generate a fragment encoding 463 bp upstream of the A5L ORF. Oligonucleotides (8) 5′-GGCATGGACGAGCTGTACAAGGACTTCTTTAACAAGTTCTCACAGGGG-3′ and (4) were used to generate a 1215 bp fragment containing the A5L ORF and 346 bp downstream of the A5L ORF. The EGFP ORF was amplified as described above. Oligonucleotides (7) and (8) contained EGFP

sequences enabling the individual fragments to be assembled into a single 2392 bp gene. This was digested with *Eco*RI and *Hin*dIII and cloned into *Eco*RI- and *Hin*dIII-digested pSJH7 to form pA5L-EGFP-N.

Revertant viruses, wherein the WT *A5L* gene was reinserted into vA5L-EGFP-C and vA5L-EGFP-N to replace the EGFP-fusion sequences, were constructed using a plasmid containing the WT *A5L* gene. This gene was amplified by oligonucleotides (1) and (4) and cloned into pSJH7 to form pA5L-rev. The fidelity of all cloned PCR products was confirmed by sequencing.

Recombinant virus construction. vA5L-EGFP and vA5L-EGFP-REV were constructed by transient dominant selection (Falkner & Moss, 1990) using the *E. coli* guanine : xanthine phosphoribosyltransferase (*Ecogpt*) gene. CV-1 cells were infected with VV WR at 0·1 p.f.u. per cell and transfected with either pA5L-EGFP-C or pA5L-EGFP-N using Lipofectin (Gibco BRL). For vA5L-EGFP-C-rev and vA5L-EGFP-N-rev, CV-1 cells were infected with either vA5L-EGFP-C or vA5L-EGFP-N and transfected with pA5L-rev. Recombinant virus expressing *Ecogpt* was selected by three rounds of plaque purification on BS-C-1 cells in the presence of mycophenolic acid (MPA). The MPA-resistant virus was then plaque-purified three times on D98R cells with 6-thioguanine to select against virus expressing Ecogpt. *Ecogpt*-negative viruses containing A5L-EGFP-C/N or A5L-EGFP-C/N-rev were identified by PCR and stocks were prepared and titrated by plaque assay on BS-C-1 cells.

Immunoblotting. IMV was purified from infected RK_{13} cells by sucrose density-gradient centrifugation as described (Mackett *et al.*, 1985). Proteins were analysed by SDS-PAGE and immunoblotting (Towbin *et al.*, 1979). A5L, EGFP and D8L were detected by rabbit α-core antibody (Cudmore *et al.*, 1996b; Vanderplasschen *et al.*, 1998) (diluted 1 : 2000), mouse mAb JL-8 (Clontech) (diluted 1 : 1000) and mouse mAb AB1.1 (Parkinson & Smith, 1994; Vanderplasschen *et al.*, 1998) (diluted 1 : 1000), respectively. Specific signals were visualized using the ECL Western blotting detection kit (Amersham).

Electron microscopy. RK_{13} cells were infected at 1 p.f.u. per cell for 8 h and were processed for thin-section transmission microscopy as described (Hollinshead *et al.*, 1999; Krauss *et al.*, 2002). For immunoelectron microscopy, ultrathin cryosections were labelled with anti-GFP (Clontech) (diluted 1 : 10). All digital images were captured with the integrated SIS image analysis package and processed using Adobe Photoshop software.

Confocal microscopy. Cells on glass coverslips were infected and at the indicated times thereafter were processed as described previously (Hollinshead *et al.*, 1999). Tetramethylrhodamine B isothiocyanate (TRITC)–phalloidin (Sigma) was used to stain F-actin and 4,6-diamine-2-phenylindole (DAPI) was added to the mounting medium to stain DNA.

For co-localization of VV cores and microtubules, PtK_2 cells on glass coverslips were infected with vA5L-EGFP-N at 0·25 p.f.u. per cell for 1 h at 37 °C. Cells were fixed with PFA at 37 °C for 10 min and permeabilized with either 0·1 % saponin or 0·1 % Triton X-100. MAbs AB1.1 (mouse, 1 : 500) and YL1/2 (rat, 1 : 1000), which detect the VV D8L protein and α-tubulin, respectively, were added for 1 h at room temperature. Bound antibodies were detected using donkey anti-mouse Cy5-conjugated and donkey anti-rat TRITC-conjugated antibodies (Jackson Immunoresearch Laboratories) diluted 1 : 100 or 1 : 400, respectively. Coverslips were mounted in Mowiol containing DAPI and were analysed using a Zeiss LSM 510 Meta confocal microscope. Images were collected and processed using LSM 510 and Adobe Photoshop software.

Time-lapse microscopy. PtK_2 cells grown to 50 % confluence on coverslips (PeCon) were infected at 0·25 p.f.u. per cell on ice for 30 min with purified vA5L-EGFP-N IMV. Where applicable, 33 μM nocodazole (Calbiochem) or 250 μM colchicine (Sigma) was added at 37 °C for 30 min before infection, or 1 μM cytochalasin D (Calbiochem) was added during infection. After binding, cells were washed with ice-cold medium and transferred to a microscope stage preheated to 37 °C. Cells were observed on the Zeiss 510 Meta confocal microscope using Zeiss time-lapse software. Images were acquired at 3 s intervals for 100 frames at different times between 0 and 90 min post-heating.

RESULTS

Genome analysis of recombinant viruses

Virus genomes were analysed by PCR using oligonucleotides that flank the *A5L* or *EGFP* gene. PCR with primers flanking the *A5L* gene produced DNA fragments of 1·6, 2·3, 2·3, 1·6 and 1·6 kb for WT, vA5L-EGFP-C, vA5L-EGFP-N, vA5L-EGFP-C-rev and vA5L-EGFP-N-rev, respectively (see supplementary data at JGV Online: http://vir.sgmjournals.org), whereas EGFP-specific primers produced a DNA fragment of 0·7 kb for vA5L-EGFP-C and vA5L-EGFP-N but not for WR or revertant viruses. The sizes of these DNA fragments confirmed that the chimaeric *vA5L-EGFP-C* and *vA5L-EGFP-N* gene was inserted into the *A5L* gene locus.

Growth properties of recombinant viruses

The isolation of each recombinant virus indicated that the fusion of EGFP to the A5L protein did not prevent virus replication. To determine if there was a growth difference between WR, A5L-EGFP-N, vA5L-EGFP-C and the revertant viruses, the yield of infectious intracellular and extracellular virus was investigated 24 h post-infection (p. i.) of BS-C-1 cells infected at 10 p.f.u. per cell. Intracellular and extracellular vA5L-EGFP-N and vA5L-EGFP-C were each reduced about 3-fold compared to WR (data not shown). Similarly, the proportion of virus released into the supernatant that was resistant to neutralization by mAb 2D5, which neutralizes IMV (Ichihashi, 1996), was indistinguishable between these viruses and WR (data not shown).

The plaque phenotype of the WR, vA5L-EGFP-C, vA5L-EGFP-N and revertant viruses was investigated under liquid or semi-solid overlay in BS-C-1 cells (Fig. 1a). Under semi-solid medium, the plaques formed by vA5L-EGFP-C were slightly smaller than WR and the revertant control, whereas plaques formed by vA5L-EGFP-N were similar to WR and revertant. With a liquid overlay virus can spread as EEV and form comets. Under these conditions, WR and the revertant viruses formed comets, but vA5L-EGFP-N and vA5L-EGFP-C did not. This result was consistent with the 3-fold reduction in EEV produced by the latter viruses.

Expression of EGFP-A5L fusion proteins in vA5L-EGFP-C and vA5L-EGFP-N

The expression of A5L-EGFP-C and A5L-EGFP-N was investigated by immunoblotting of infected cell lysates (data not shown) and purified IMV (Fig. 1b). Extracts from WR, vA5L-EGFP-C and vA5L-EGFP-N IMV were blotted with

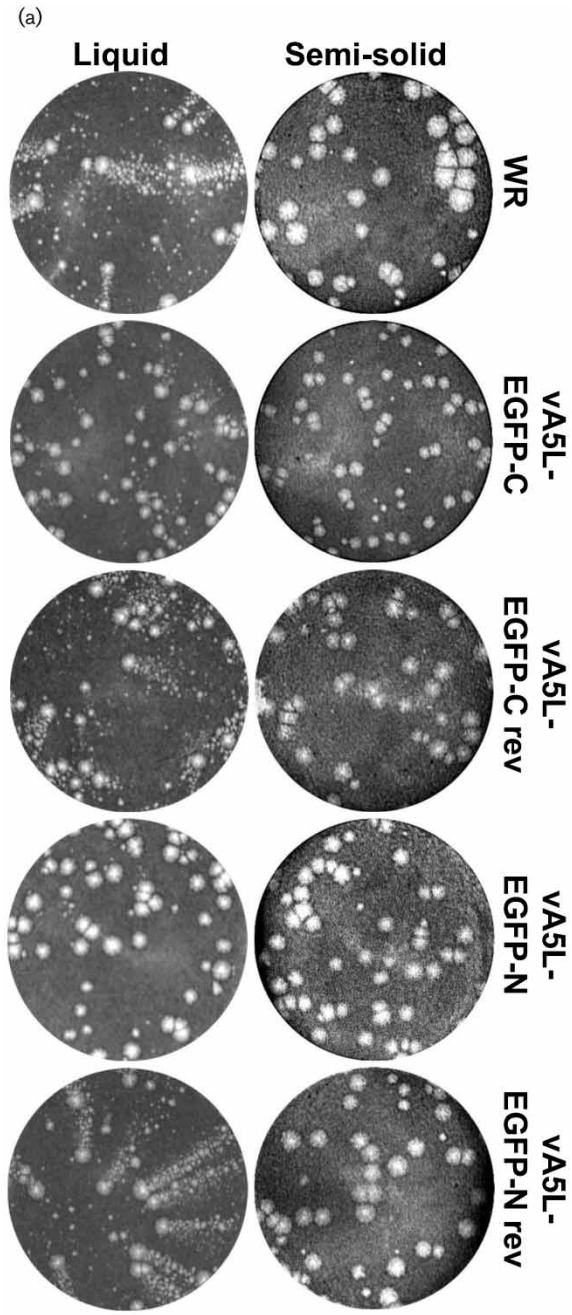

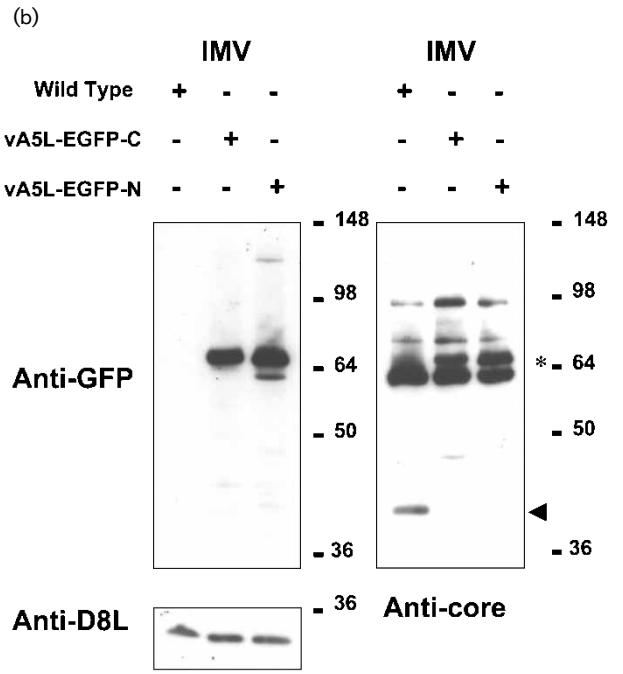

Fig. 1. (a) Plaque phenotypes. BS-C-1 cells were infected with the viruses indicated and incubated under semi-solid or liquid medium for 3 days. The medium was removed and cells were stained with 0·1% crystal violet in 15% ethanol. (b) Immunoblot showing A5L-EGFP incorporation into IMV. IMV were purified from RK_{13} cells infected with the indicated viruses. Proteins were detected with mouse mAb JL-8, (anti-EGFP), mouse mAb Ab1.1 (anti-D8L) or rabbit antiserum raised against core antigens. The positions of molecular size markers are shown in kDa.

antibody to either VV core proteins or GFP. A protein of 67 kDa was detected by anti-GFP mAb in each recombinant VV but not in WR. This size was consistent with the addition of EGFP to the 39 kDa A5L protein. As a loading control, the blot was probed with α-D8L mAb and this detected D8L protein at a similar level in each virus preparation. Using the anti-core antibody, the major core protein of about 39 kDa in WR (arrowhead) was replaced with a protein of about 67 kDa (star) in both recombinant viruses. The higher molecular mass species present in the A5L-EGFP-N protein probably represents oligomeric forms of this protein. These data showed that each chimaeric A5L-EGFP protein was synthesized and packaged into IMV particles.

Location of EGFP-A5L fusion proteins in infected cells

Fig. 1(b) suggested that the A5L-EGFP-C and A5L-EGFP-N proteins were incorporated into VV particles. This was investigated further by confocal microscopy to analyse the distribution of these fusion proteins in infected cells (Fig. 2). In cells infected with vA5L-EGFP-C, direct visualization of EGFP showed punctate structures distributed throughout the cell (panel a). If the cell was also stained with DAPI for DNA (panel b) and the image merged (inset), it was evident that these EGFP-positive structures contained DNA and therefore are very likely to be virions. Analysis with vA5L-EGFP-N gave similar data (data not shown). In addition, to investigate if cells infected with vA5L-EGFP-N formed actin tails, cells were stained with phalloidin (panel d) and merged with an image of EGFP fluorescence (panel c). Panel (d) shows the presence of many actin tails and the inset shows a merged image demonstrating that the actin tails each have a virus particle at their tip.

Electron microscopy

The location of the A5L-EGFP fusion protein was also investigated by electron microscopy (Fig. 3). Analysis of

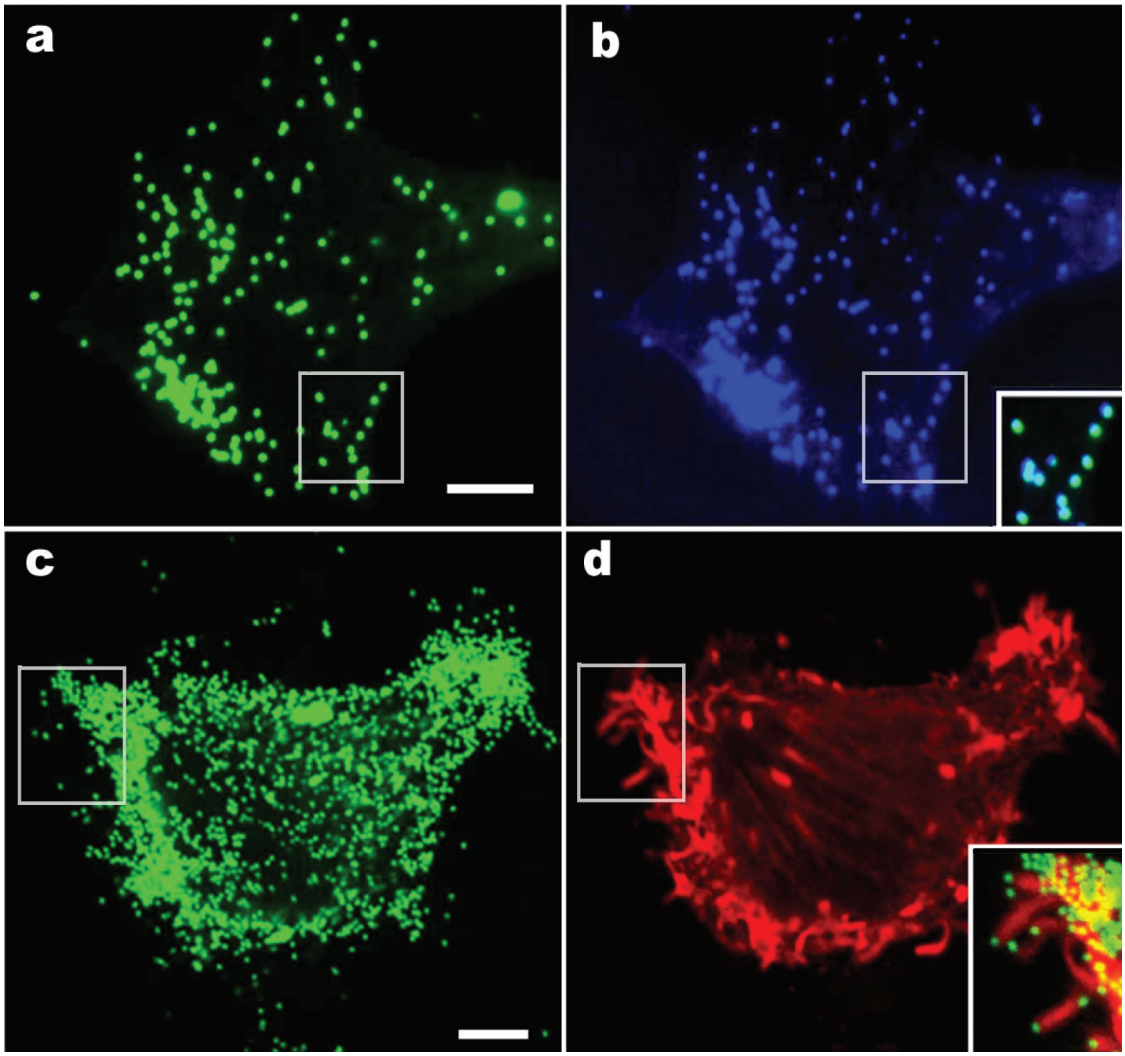

Fig. 2. Location of vA5L-EGFP in infected cells and virus-induced actin tail formation. BS-C-1 cells were infected at 1 p.f.u. per cell with vA5L-EGFP-C (a and b) or at 10 p.f.u. per cell with vA5L-EGFP-N (c and d) and were processed for confocal microscopy. At 12 h p.i. virus particles were visualized directly by virtue of the EGFP (a) and staining with DAPI (b). The insert in panel (b) shows an enlarged and merged area that is boxed in (a) and (b). (c and d) At 14 h p.i. virus particles were visualized by virtue of EGFP (c) and actin tails were revealed by staining with TRITC–phalloidin (d). An enlarged and merged area that is boxed in (c) and (d) is shown in the insert. Scale bar, 5 μm.

thin sections of vA5L-EGFP-N-infected cells revealed that virus morphogenesis was normal and within virus factories it was possible to detect virus crescents and immature virus particles (Fig. 3a, b). Furthermore, complete IEV particles and IMV particles that were being wrapped to form IEV were visible within the cell (panel c). CEV particles were visible on the cell surface or on the tip of actin tails protruding from the cell surface (panel d). To determine if A5L-EGFP-N was associated with these structures, cryosections of infected cells were treated with α-EGFP mAb followed by a protein A–gold conjugate. Gold particles were visible within the core, within the area surrounded by crescents, immature virions (Fig. 3e, f) and with IMVs (panel g). The distribution of these gold particles contrasted with those used to detect the B5R-EGFP fusion protein around IEV or on the surface of CEV (panel h). In addition, we analysed the location of A5L-EGFP-N on cores released into the cytosol after infection with vA5L-EGFP-N and found it was on the surface of cores (data not shown), and indistinguishable from wild-type A5L (Pedersen *et al.*, 2000). Collectively, these data show that virus morphogenesis is normal and the A5L-EGFP-N protein is incorporated into the virus core. Similar data were obtained for A5L-EGFP-C (data not shown).

Visualization of intracellular cores

To use the vA5L-EGFP viruses for studies of virus entry and core movement, IMV were bound to cells on ice, the

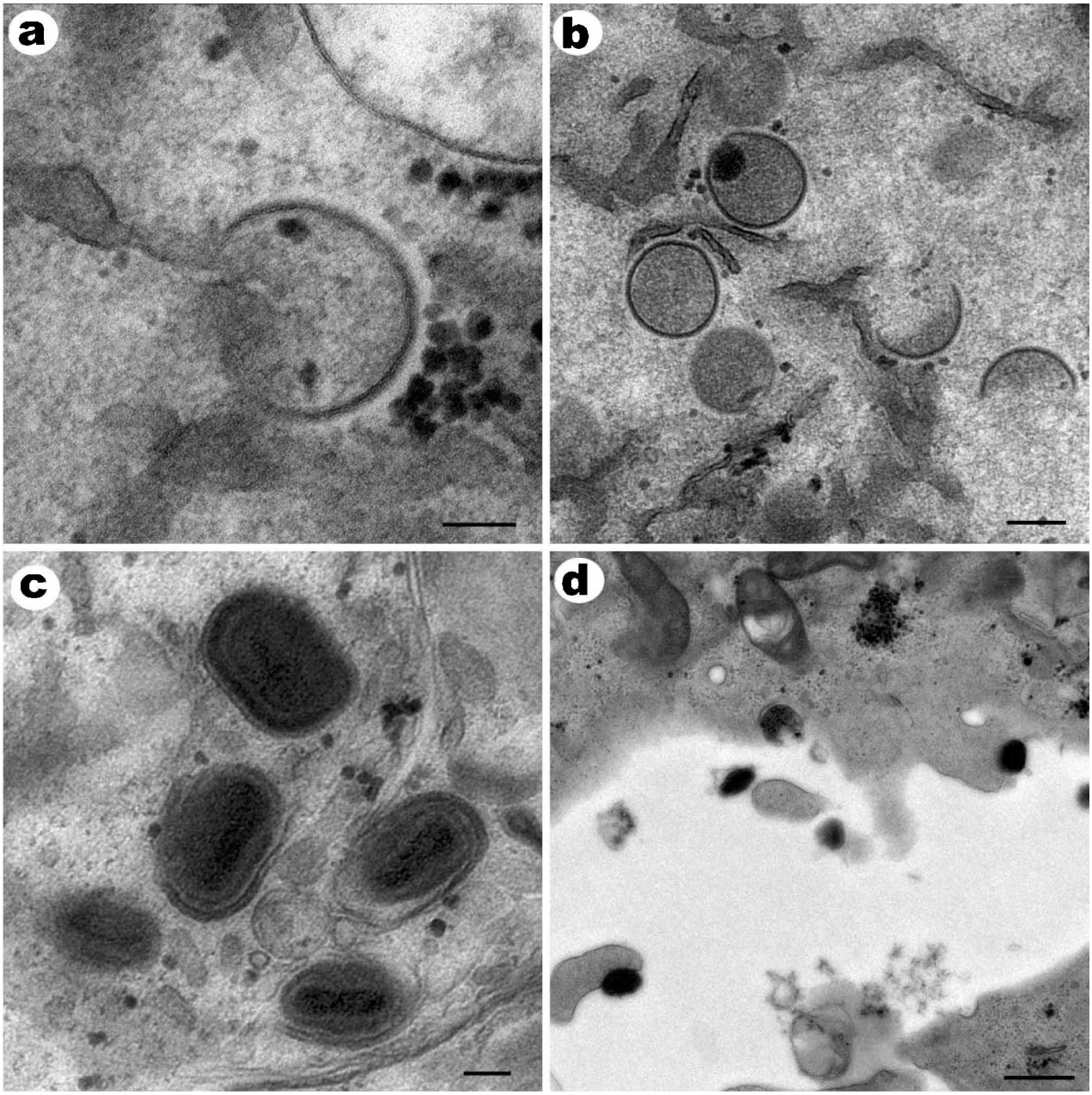

cells were warmed to 37 °C and virions were visualized by staining with anticore antibody (Fig. 4a), EGFP fluorescence (Fig. 4b) or mAb to the IMV surface protein D8L (Fig. 4c). All particles were visible by EGFP (including those bound to the coverslip) whereas only a subset were recognized by anti-core antibody or anti-D8L. All structures positive for core antigens were also positive for EGFP, and the majority (68·8 %) of these were negative for D8L (Fig. 4d, merged image), consistent with loss of D8L on entry. The few triple-positive structures are probably cores that have entered the cell but not moved from the entry point where the D8L envelope remains, rather than cores on the cell surface, because the anti-core antibody only stains intracellular cores (Vanderplasschen *et al.*, 1998; Krijnse Locker *et al.*, 2000). This is addressed further below. When virions were bound onto cells on ice and visualized directly, no cores were visible (data not shown).

To demonstrate that the core-positive structure had entered the cell, further co-localization studies were performed. vA5L-EGFP-N was added to Ptk_2 cells and incubated for 1 h at either 37 or 4 °C. Virus particles were detected using anti-D8L mAb and microtubules were revealed using anti-tubulin mAb. At 37 °C, many EGFP-positive and D8L-negative virus particles were observed (Fig. 5e, green particles). One such particle is arrowed, indicating that the vA5L-EGFP-N has lost its IMV membrane and the green particles are likely to be intracellular cores (Fig. 5a, c, k, l). When projections of *Z*-series images were examined in the orthogonal plane, EGFP-positive core particles (Fig. 5a, arrowhead) that did

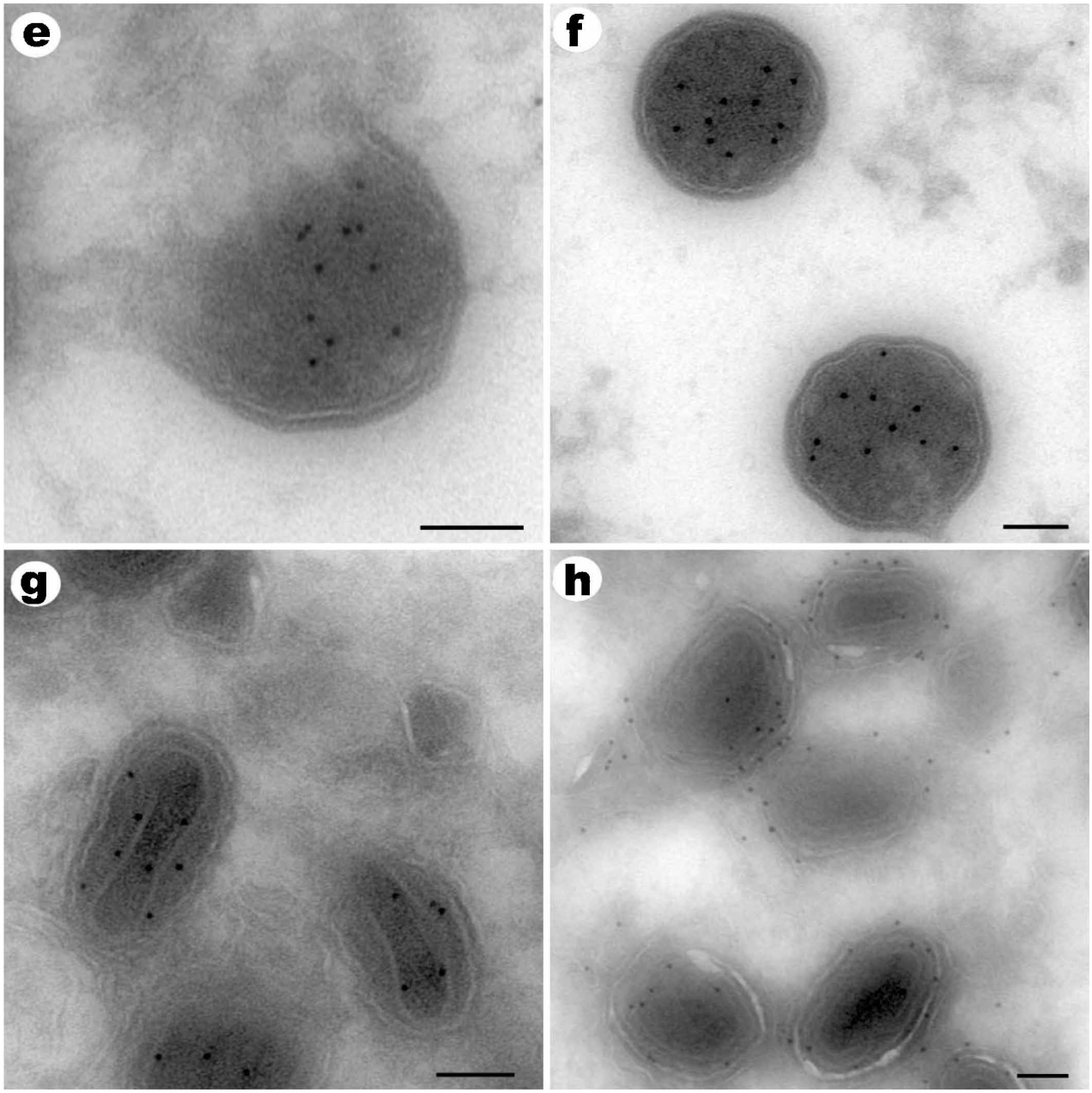

Fig. 3. Electron microscopy. (a–d) RK_{13} cells were infected with vA5L-EGFP-N at 1 p.f.u. per cell and at 8 h p.i. samples were processed for conventional transmission electron microscopy of Epon sections. Images show a single crescent (a), immature viruses (b), IMV and IEV (c) and CEV (d). (e–h) RK_{13} cells were infected with vA5L-EGFP-N at 1 p.f.u. per cell (e–g) or vB5R-GFP (h) (Hollinshead *et al*., 2001). Samples were processed for cryo-electron microscopy as described in Methods. Sections were incubated with mAb JL-8 against GFP followed by protein A–gold conjugates. Note the presence of A5L-EGFP within the cores of IV and mature virus (e, f, g) whereas the B5R-EGFP protein is located on the wrapping membranes of IEV and CEV (h). Scale bars for panels (a), (c), (e)–(h), 100 nm; (b), 200 nm; (d), 500 nm.

not label with anti-D8L (Fig. 5c, arrowhead) were observed in the perinuclear region close to the bottom of the cell and surrounded by microtubules (Fig. 5g, i, k, l). At 4 °C, all the virions on or around the cell are positive for EGFP and D8L (Fig. 5 right column, arrowheads and panels m, n). Moreover, when Z-series sections were examined in the orthogonal plane such virions were located on the surface of the cell (Fig. 5h, j, arrowheads). Together these data indicate that vA5L-EGFP-N loses its IMV membrane upon entry and only the core is transported after the entry process.

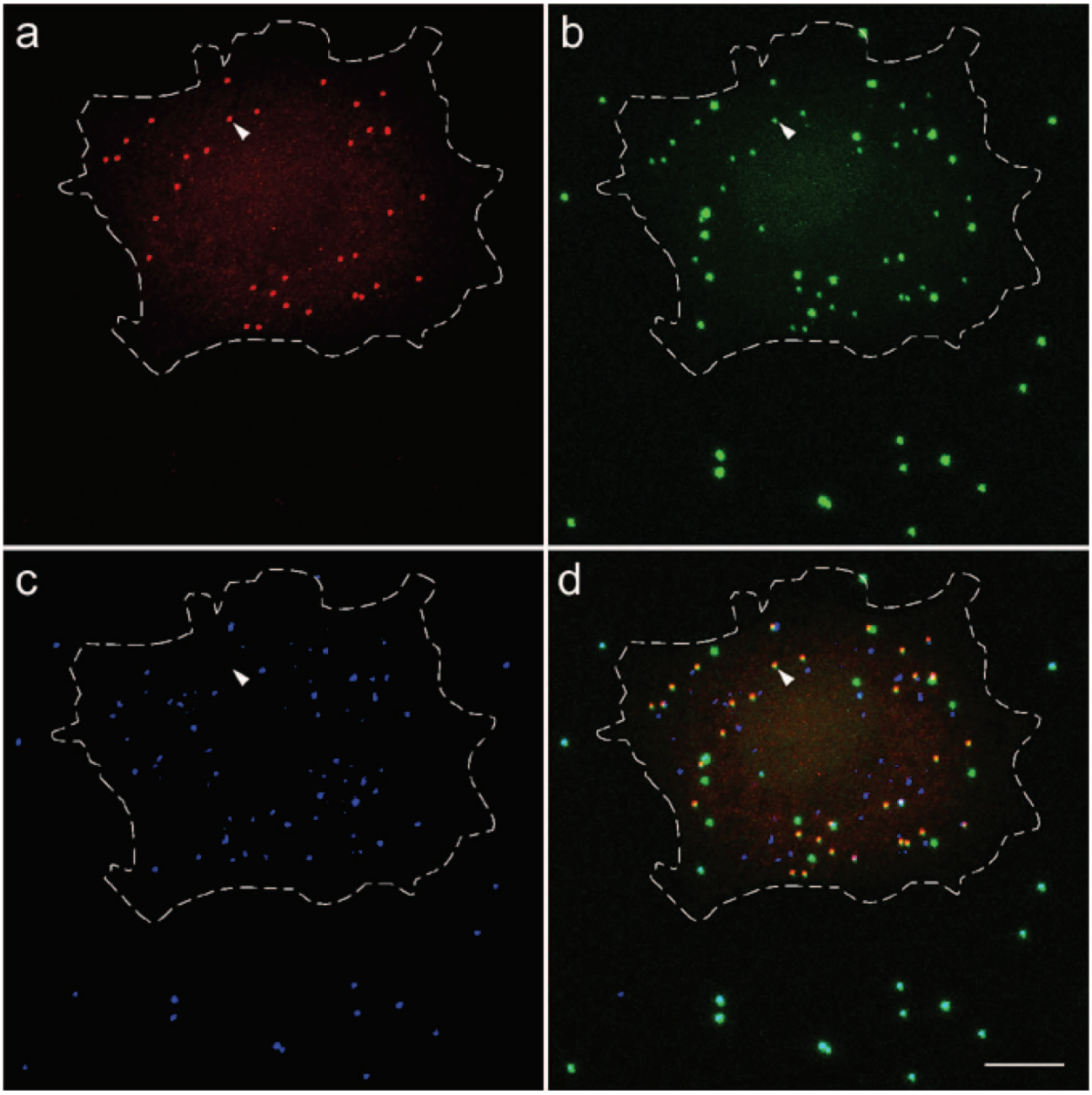

Fig. 4. Colocalization of A5L-EGFP-N with core antigens. Ptk2 cells were bound with purified IMV of vA5L-EGFP-N for 1 h on ice and then at 37 °C for 30 min to allow virus entry. The infected cells were permeabilized and stained with anti-core antibody (a) and anti-IMV mAb AB1.1 (c). EGFP fluorescence is shown in (b) and a merged image of panels (a)–(c) is shown in (d). Projected *Z*-series confocal images ($n=12$, 0·35 μm section) are shown and the cell boundary is outlined. Scale bar, 10 μm.

The location of cores relative to the microtubule network was examined from the data shown in Fig. 5 and other cells (not shown). At 37 °C, 80 % of particles were cores (EGFP-positive and D8L-negative) and the majority of these 83 % ($n=100$) were coincident with α-tubulin. At 4 °C (when free cores are not formed) no D8L-negative particles were seen, but the majority (63 %) of IMV particles were still proximal to microtubules.

Movement of EGFP-cores observed by time-lapse microscopy

Purified IMV from vA5L-EGFP-N was used to investigate how virus cores move within a newly infected cell. IMV was bound on ice to PtK_2 cells, which have a large flat morphology and so are useful for time-lapse microscopy. After binding, cells were warmed to 37 °C and analysed at

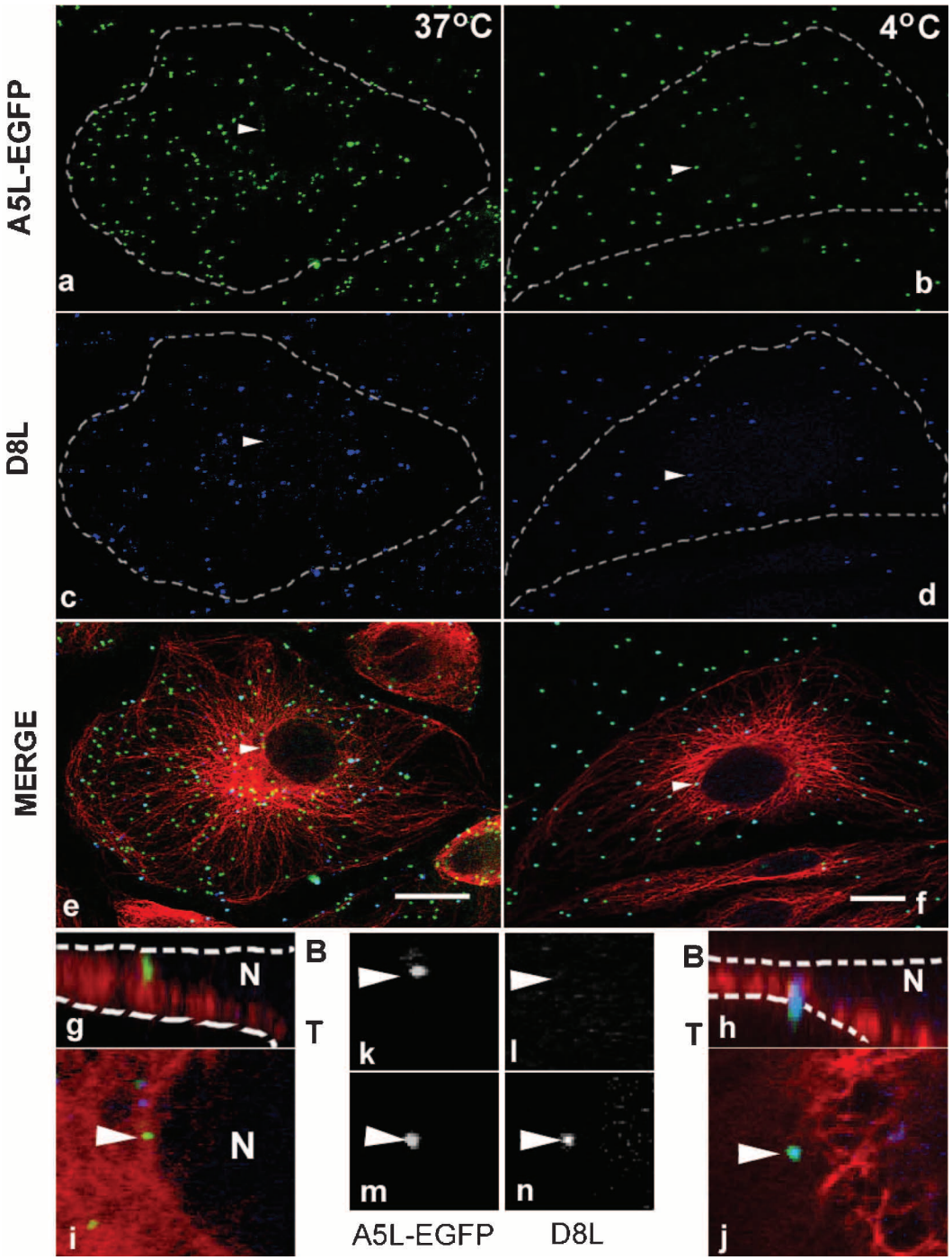

Fig. 5. Intracellular location of vA5L-EGFP-N cores. PtK_2 cells were incubated with vA5L-EGFP-N for 1 h at either 4 or 37 °C and then processed for immunofluorescence using either EGFP (a, b), mouse mAb AB1.1 to detect D8L protein (c, d) or rat mAb YL1/2 to detect α-tubulin (e, f). Bound mAbs were detected by Cy5–donkey anti-mouse antibody or TRITC–donkey anti-rat antibody. The cell outlines are indicated by the broken line. Panels (e) and (f) include tubulin staining and a merge of the TRITC and EGFP signals; panels (g) and (h) show orthogonal projected *Z*-series images ($n=17$, 0·38 μm section) of panels (e) and (f) respectively. Bar, 10 μm. Note the location of the EGFP-positive core at 37 °C close to the bottom of the cell and the presence of the double-positive IMV particle on the surface of the cell at 4 °C. Enlarged single optical sections of the same region showing a merge of the TRITC and EGFP signals are shown in panels (i) and (j). Single channel panels of EGFP (k, m) or D8L (l, n) are shown. Note the lack of D8L signal when the virus was incubated at 37 °C (l) compared to the presence of the D8L signal when incubated at 4 °C (n). B, bottom of cell; T,: top of cell; N, nucleus. Scale bar, 10 μm.

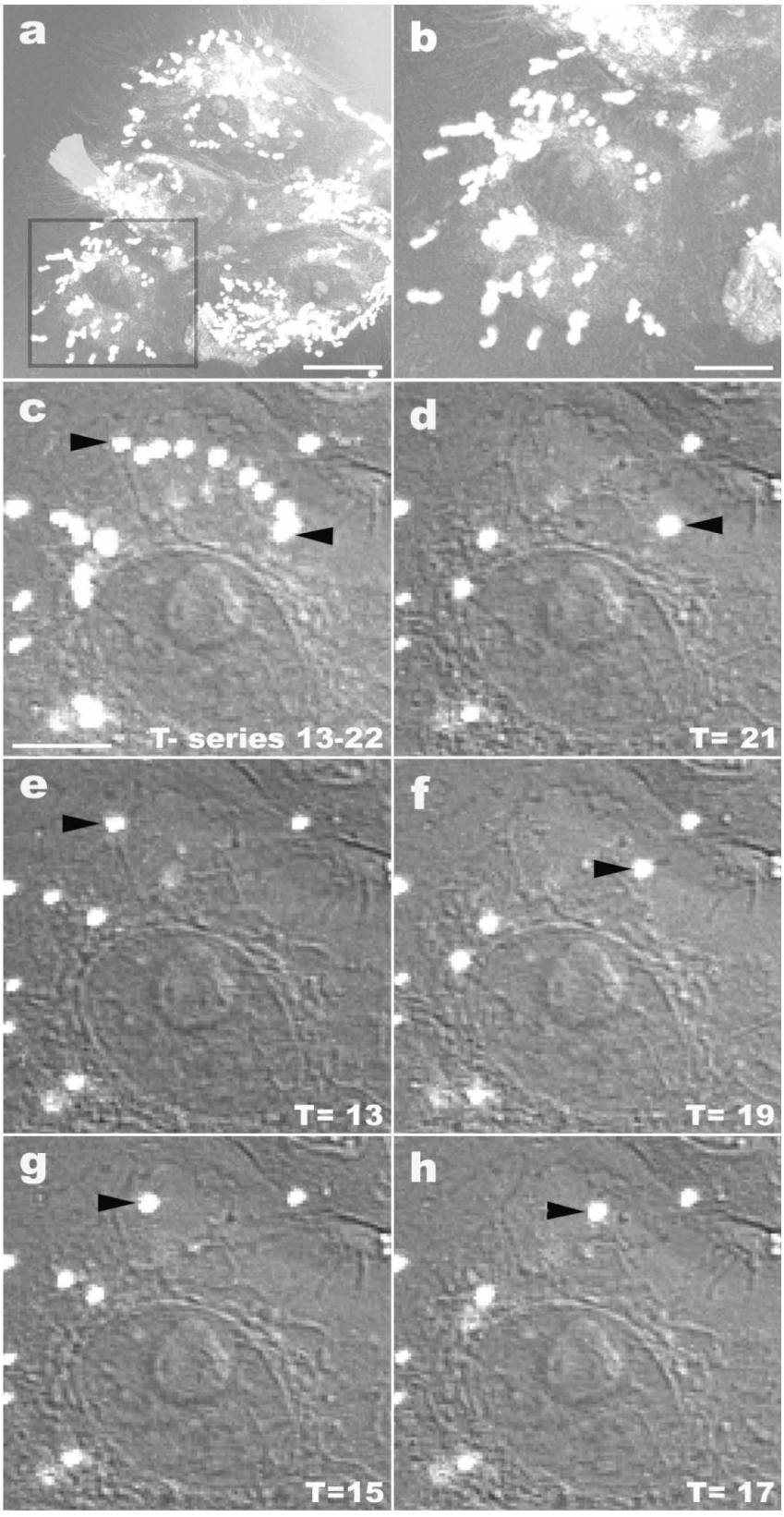
a
b
c
T- series 13-22
d
T= 21
e
T= 13
f
T= 19
g
T=15
h
T= 17

different times post-warming by confocal microscopy with a series of 100 images captured every 3 s. A representative experiment is shown in Fig. 6. In panel (a), the direct fluorescence deriving from EGFP in a single focal plane at all 100 time-points is shown. Part of this image is shown at higher magnification in panel (b). It is evident that many of the virus particles exhibit little movement as their images remain reasonably stationary over the 300 s period. This may be because they have already entered and moved, or they may not have entered the cell and may move at a later stage. However, several particles showed clear movement. This is illustrated in the remaining images. Arrowheads in panel (c) show the position of a single particle between frames 13 to 22. In panels (e), (g), (h), (f) and (d) the position of this particle at 6 s intervals is illustrated by an arrowhead. Particles were seen moving in a saltatory manner both towards and away from the perinuclear region. Time-lapse analyses of multiple particles ($n=20$) showed particles moved with speeds ranging from 27 to 80 μm min^{-1} (average 51·8 μm min^{-1}, SEM ± 3·9 μm min^{-1}). These types of movement and speeds are consistent with movement on microtubules.

To investigate this further, the effects of the microtubule-disrupting drugs nocodazole and colchicine were analysed. Time-lapse confocal images were taken every 3 s for 5 min at 30 min after warming and the merged images are shown in Fig. 7. In the presence of colchicine (a) or nocodazole (c) the great majority of individual particles remained punctate due to lack of movement, but after washout of nocodazole (b) movement was restored. During a 5 min period (25–30 min p.i.) the number of particles moving on microtubules at speeds ⩾27 μm min^{-1} (the lowest rate of movement without drug) from ten cells was analysed. In the absence of drugs 19·7 % of particles ($n=250$) moved, but this was reduced to 1·2 % ($n=167$) and 0·6 % ($n=201$) in the presence of colchicine and nocodazole, respectively. Upon nocodazole washout 15·1 % ($n=253$) of particles moved. In the presence of cytochalasin D (panel d), an actin-disrupting drug, 14·3 % ($n=215$) of particles moved. Panels (e) and (f) show the movement of a single particle after nocodazole washout and in the presence of cytochalasin D, respectively. The rate of particle movement ($n=20$) was also measured in the presence of cytochalasin D and after nocodazole washout. Cytochalasin D did not inhibit the rate of movement (average 51·0 ± 5·3 μm min^{-1}), although the number of cores moving was reduced slightly. The effect of nocodazole was reversible and after drug washout movement was restored (average 54·2 ± 3·3 μm min^{-1}).

Distributions of virions on the cell

To investigate whether the cores move from the cell periphery to the cell interior, serial optical sections of the infected cells were collected. After virus binding to cells at 4 °C, cells were warmed to 37 °C, and *X*–*Y* sections were taken of a group of cells at different times thereafter (Fig. 8). Analysis of these projected *X*–*Y* sections revealed that shortly after infection (10 min) the EGFP-positive particles are distributed randomly over the cell surface. At later times during infection (70 and 100 min) the majority of particles were seen to concentrate around or above the nucleus and to have more variable intensity. This change in distribution was inhibited by nocodazole (data not shown). These observations are consistent with virions moving from the cell periphery to the more central region of the cell and suggest some may already have started to disassemble further.

DISCUSSION

This report describes the construction and use of recombinant VVs in which the *A5L* gene was replaced with the *A5L* gene fused to EGFP-coding sequences at the 5′ or 3′ end. Cores derived from these recombinant viruses after infection of new cells moved with speeds consistent with transport on microtubules. Moreover, movement of cores was inhibited by drugs that disrupt microtubules but not by drugs that disrupt actin filaments. Thus VV uses microtubules for transport of both incoming cores and outgoing particles.

Previously, recombinant VVs were described in which the F13L or B5R proteins were fused to GFP or EGFP and these viruses were useful for studying the movement of IEV particles during virus egress. However, these viruses could not be used for studying movement of IMV particles during morphogenesis, or virus cores during re-infection, because the virus particles only acquired the EGFP-tagged protein after formation of IEV during morphogenesis and the EGFP tag was lost during re-entry because it was present in the EEV outer envelope. To overcome this problem we sought a core protein that might be tagged with EGFP without inhibiting function and selected the *A5L* gene for study. Although this gene is essential for virus morphogenesis and

Fig. 6. Visualization of core movement by time-lapse confocal microscopy. vA5L-EGFP-N purified IMV were bound to PtK_2 cells on ice for 30 min and then transferred to a Zeiss 510 Meta confocal microscope preheated to 37 °C. Time-series images were collected every 3 s for 100 frames at 50 min post-heating. Virus particles were visualized by virtue of EGFP and cell morphology was observed by differential interference contrast (DIC) microscopy. (a) The 100 time-series frames were projected to create images showing all virus movement. (b) Region of (a) enlarged to show a single cell. (c) Movement of a single core over ten 3 s intervals (frames 13–22) tracked in a projection. Arrows indicate first and last positions. (d–h) The individual movements of this particle at 6 s intervals are indicated by the arrow at frame 13 (e), 15 (g), 17 (h), 19 (f) and 21 (d). This core moves 13·3 μm in 27 s equivalent to be a speed of 29·5 μm min^{-1}. Scale bars, 20 μm for panel (a); 10 μm for panel (b); 5 μm for panels (c)–(h).

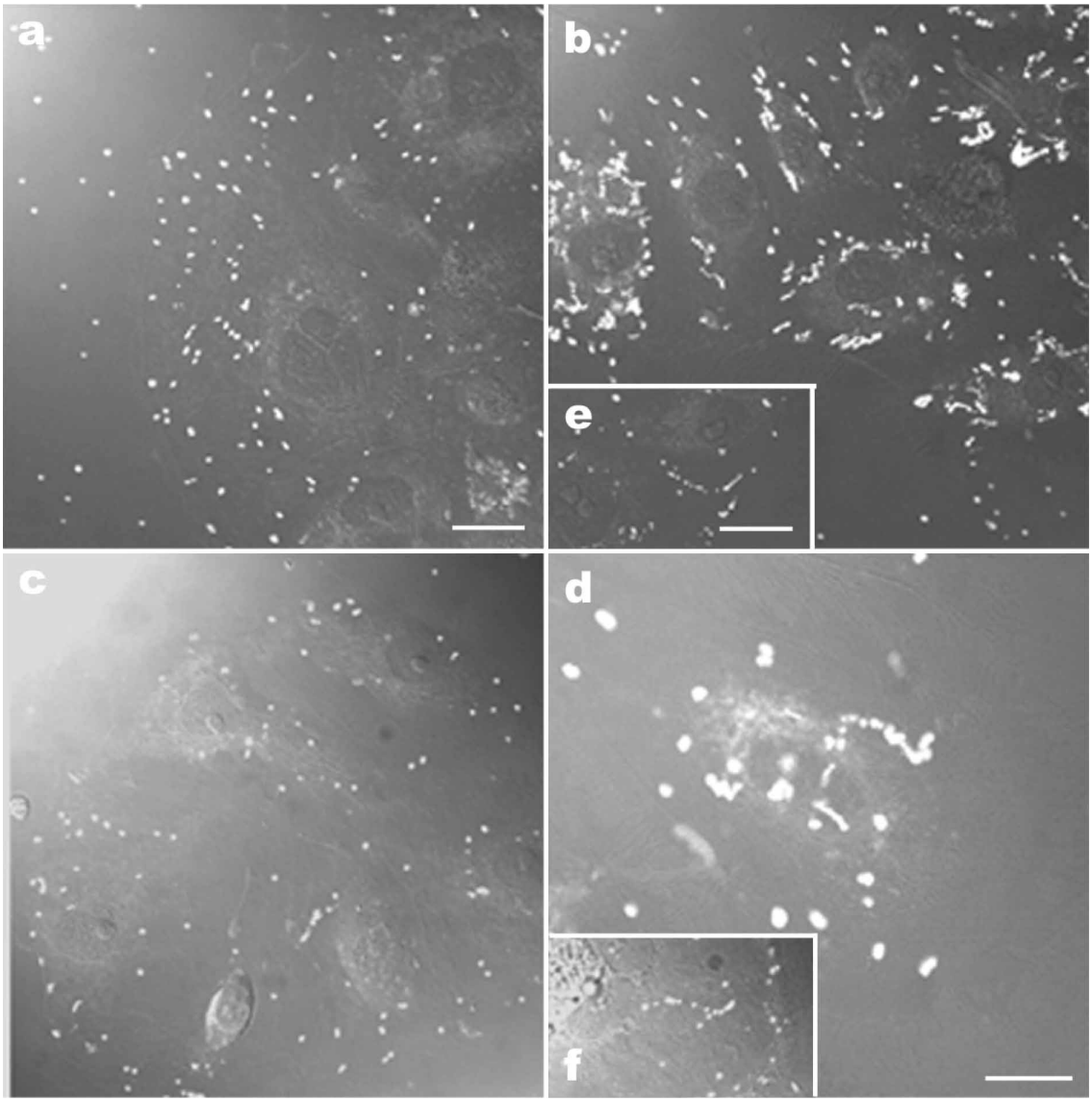

Fig. 7. Effects of microtubule- and actin-disrupting drugs. PtK_2 cells were treated with 33 μM nocodazole or 250 μM colchicine for 30 min at 37 °C before infection, while no pretreatment was done with cytochalasin D (1 μM). Purified IMV from vA5L-EGFP-N at 0·25 p.f.u. per cell was bound onto the cells for 30 min on ice in the presence of drug. Cytochalasin D (1 μM) was incubated with cells during the virus-binding stage. The cells were transferred to a Zeiss 510 Meta confocal microscope at 37 °C and time-series images were collected at 30 min post-heating every 3 s for 100 frames. Cells remained in the presence of drugs during confocal analysis. Virus particles were visualized by virtue of EGFP and cell morphology was observed by DIC microscopy. The time-series frames were merged to create images showing all virus movement. (a) Nocodazole at 31 min p.i; (b) 26 min after nocodazole washout; (c) colchicine at 33 min p.i.; (d) cytochalasin D at 27 min p.i. (b) After preincubation in nocodazole, cells were incubated at 37 °C with nocodazole for 45 min, the drug was then washed out and images were collected 26 min later. Panels (e) and (f) show movement of a single particle after nocodazole washout (e) and cytochalasin D treatment (f). Scale bars, 20 μm for (a)–(d); 10 μm for (e)–(f).

the morphogenesis of a mutant virus in which expression of the gene is repressed arrests prior to the formation of IMV, we were able to replace the wild-type *A5L* gene with A5L fused to EGFP at either the N or C terminus and recover infectious virus. Moreover, immunoblotting of proteins extracted from purified IMV showed the protein was present in IMV particles, and cryo-immunoelectron microscopy showed that the A5L-EGFP fusion proteins were incorporated into the virus core. These observations suggest that interactions of the A5L protein via either the N or C terminus is not critical for functions such as packaging into virions or interaction with other proteins.

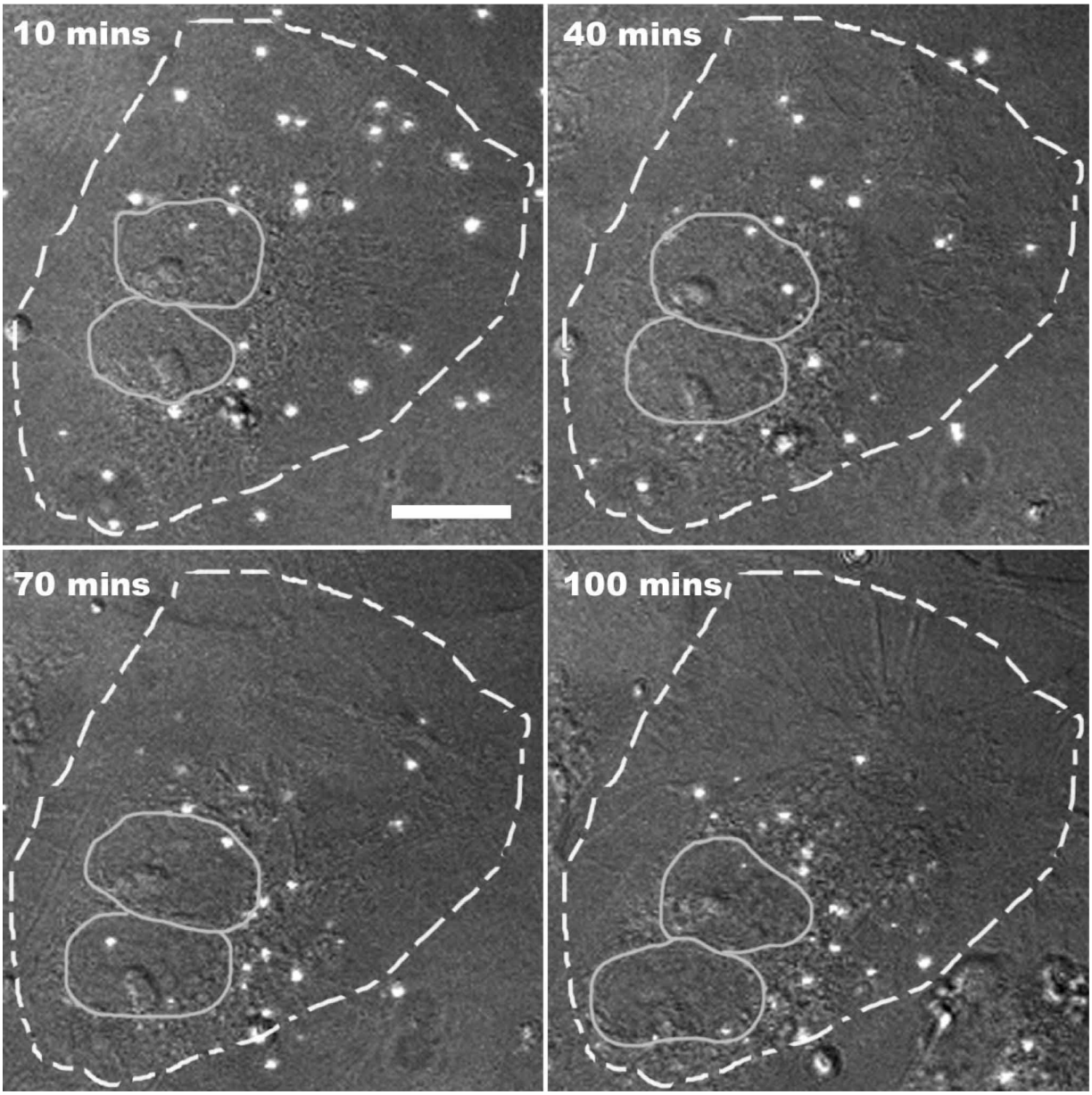

Fig. 8. Distribution of virions on the cell. vA5L-EGFP-N purified IMV were bound to PtK_2 cells on ice for 30 min and then transferred to a Zeiss 510 Meta confocal microscope preheated to 37 °C. Optical *X*–*Y* sections (*Z*-stack images) were taken of a group of cells every 15 min for 100 min. Projections of the optical sections are shown (a) 10 min post-heating, (b) 40 min post-heating, (c) 70 min post-heating and (d) 100 min post-heating. Scale bar, 5 μm.

Electron microscopy showed that recombinant viruses expressing the A5L-EGFP fusion proteins underwent normal morphogenesis and induced the formation of virus-tipped actin tails at the cell surface. Consistent with this observation, the plaque size of the recombinant viruses was similar to or indistinguishable from wild-type and revertant virus controls. The virus with the EGFP fused to the C terminus formed a slightly smaller plaque than the wild-type.

Immunofluorescent microscopy showed that IMV particles bound to the cell surface retained the D8L IMV surface protein, but were not recognized by the anti-core antibody. Conversely, particles that had entered the cell were recognized by core antibody but not antibody to D8L. Both observations are in accord with a previous report (Vanderplasschen *et al.*, 1998) and are relevant to the entry mechanism for IMV. It was proposed that IMV uncoats outside the cell followed by transport of cores across the cell membrane without membrane fusion (Krijnse Locker *et al.*, 2000). The failure to detect cores on the cell surface is

inconsistent with this proposal, unless cores somehow remain inaccessible to anti-core antibody once released from the IMV membrane. Particles that had entered the cell moved from the cell periphery towards the cell interior and co-localized with α-tubulin. This co-localization of virus cores with microtubules is consistent with a previous report (Mallardo *et al.*, 2001) that also noted co-localization of virus mRNAs and microtubules.

The movement of cores derived from IMV was followed by time-lapse confocal microscopy after infection of new cells, and cores were found to move with speeds consistent with transport on microtubules. Moreover, addition of either colchicine or nocodazole inhibited core movement, and the washout of nocodazole restored core movement. These observations too are consistent with movement on microtubules. In contrast, addition of cytochalasin D, an inhibitor of actin function, did not prevent movement of cores. However, cytochalasin D did reduce the number of cores (25 % less) moving within cells, although the rate of movement was not altered. This reduction in intracellular cores in the presence of cytochalasin D is less than reported previously (81 %) (Vanderplasschen *et al.*, 1998) because of the lower drug concentration and shorter incubation period with drug in PtK_2 cells. The role of actin in IMV entry reported by Vanderplasschen *et al.* (1998) was later confirmed and extended by Krijnse Locker *et al.* (2000) who also reported the formation of cell surface projections upon binding of IMV to cells.

The use of microtubules for movement of (i) IMV particles from virus factories to sites of wrapping to form IEV, (ii) IEV particles to the cell surface and (iii) virus cores from the periphery to the cell interior illustrates how VV exploits the cell transport processes for its intracellular transport. The proteins that interact with microtubules are not defined but are likely to be different between IMV, IEV and cores. Candidate proteins include the IMV surface protein A27L and the IEV surface protein F12L. In the absence of A27L IMV are formed but not transported (Rodriguez & Smith, 1990); similarly, in the absence of F12L IEV are formed but not transported (van Eijl *et al.*, 2002). The A36R protein has also been reported to have a role in movement of IEV particles on microtubules (Rietdorf *et al.*, 2001) but EEV and CEV are still formed by viruses lacking A36R (Introduction). For incoming virus cores, the A27L and F12L proteins are absent and so other VV proteins are likely to be involved. *In vitro* microtubule-binding assays have suggested an interaction between L4R and A10L and microtubules (Ploubidou *et al.*, 2000), but these proteins are considered to be within the core rather than on its surface, and so it is uncertain how such an interaction would be mediated.

Lastly, VV is another virus shown to use microtubules during virus entry. Others include herpes simplex virus (Sodeik *et al.*, 1997), adenovirus (Suomalainen *et al.*, 1999) and HIV-1 (McDonald *et al.*, 2002). It is probable that many viruses including those described to date (Sodeik, 2000) will utilize aspects of the cell transport machinery to facilitate entry of incoming cores or capsids.

ACKNOWLEDGEMENTS

This work was supported by The Wellcome Trust, the U.K. Medical Research Council and the European Community. G. L. S. is a Wellcome Trust Principal Research Fellow.

REFERENCES

Blasco, R. & Moss, B. (1991). Extracellular vaccinia virus formation and cell-to-cell virus transmission are prevented by deletion of the gene encoding the 37,000-Dalton outer envelope protein. *J Virol* **65**, 5910–5920.

Cudmore, S., Cossart, P., Griffiths, G. & Way, M. (1995). Actin-based motility of vaccinia virus. *Nature* **378**, 636–638.

Cudmore, S., Reckmann, I., Griffiths, G. & Way, M. (1996a). Vaccinia virus: a model system for actin–membrane interactions. *J Cell Sci* **109**, 1739–1747.

Cudmore, S., Blasco, R., Vincentelli, R., Esteban, M., Sodeik, B., Griffiths, G. & Krijnse Locker, J. (1996b). A vaccinia virus core protein, p39, is membrane associated. *J Virol* **70**, 6909–6921.

Dales, S. & Siminovitch, L. (1961). The development of vaccinia virus in Earles L strain cells as examined by electron microscopy. *J Biophys Biochem Cytol* **10**, 475–503.

Demkowicz, W. E., Maa, J. S. & Esteban, M. (1992). Identification and characterization of vaccinia virus genes encoding proteins that are highly antigenic in animals and are immunodominant in vaccinated humans. *J Virol* **66**, 386–398.

Falkner, F. G. & Moss, B. (1990). Transient dominant selection of recombinant vaccinia viruses. *J Virol* **64**, 3108–3111.

Frischknecht, F., Moreau, V., Röttger, S., Gonfloni, S., Rechmann, I., Superti-Furga, G. & Way, M. (1999). Actin-based motility of vaccinia virus mimics receptor tyrosine kinase signalling. *Nature* **401**, 926–929.

Geada, M. M., Galindo, I., Lorenzo, M. M., Perdiguero, B. & Blasco, R. (2001). Movements of vaccinia virus intracellular enveloped virions with GFP tagged to the F13L envelope protein. *J Gen Virol* **82**, 2747–2760.

Goebel, S. J., Johnson, G. P., Perkus, M. E., Davis, S. W., Winslow, J. P. & Paoletti, E. (1990). The complete DNA sequence of vaccinia virus. *Virology* **179**, 247–266.

Griffiths, G., Roos, N., Schleich, S. & Krijnse Locker, J. (2001a). Structure and assembly of intracellular mature vaccinia virus: thin-section analyses. *J Virol* **75**, 11056–11070.

Griffiths, G., Wepf, R., Wendt, T., Krijnse Locker, J., Cyrklaff, M. & Roos, N. (2001b). Structure and assembly of intracellular mature vaccinia virus: isolated-particle analysis. *J Virol* **75**, 11034–11055.

Hollinshead, M., Vanderplasschen, A., Smith, G. L. & Vaux, D. J. (1999). Vaccinia virus intracellular mature virions contain only one lipid membrane. *J Virol* **73**, 1503–1517.

Hollinshead, M., Rodger, G., van Eijl, H., Hollinshead, R., Law, M., Vaux, D. T. & Smith, G. L. (2001). Vaccinia virus utilizes microtubules for movement to the cell surface. *J Cell Biol* **154**, 389–402.

Horton, R. M., Cai, Z. L., Ho, S. N. & Pease, L. R. (1989). Gene splicing by overlap extension: tailor-made genes using the polymerase chain reaction. *Biotechniques* **8**, 528–535.

Hughes, S. J., Johnston, L. H., de Carlos, A. & Smith, G. L. (1991). Vaccinia virus encodes an active thymidylate kinase that complements a cdc8 mutant of *Saccharomyces cerevisiae*. *J Biol Chem* **266**, 20103–20109.

Husain, M. & Moss, B. (2001). Vaccinia virus F13L protein with a conserved phospholipase catalytic motif induces colocalization of the B5R envelope glycoprotein in post-Golgi vesicles. *J Virol* **75**, 7528–7542.

Ichihashi, Y. (1996). Extracellular enveloped vaccinia virus escapes neutralization. *Virology* **217**, 478–485.

Katz, E., Wolffe, E. & Moss, B. (2002). Identification of second-site mutations that enhance release and spread of vaccinia virus. *J Virol* **76**, 11637–11644.

Krauss, O., Hollinshead, R., Hollinshead, M. & Smith, G. L. (2002). An investigation of the incorporation of cellular antigens in vaccinia virus particles. *J Gen Virol* **83**, 2347–2359.

Krijnse Locker, J., Kuehn, A., Schleich, S., Rutter, G., Hohenberg, H., Wepf, R. & Griffiths, G. (2000). Entry of the two infectious forms of vaccinia virus at the plasma membrane is signaling-dependent for the IMV but not the EEV. *Mol Biol Cell* **11**, 2497–2511.

Law, M., Hollinshead, R. & Smith, G. L. (2002). Antibody-sensitive and antibody-resistant cell-to-cell spread of vaccinia virus: role of the A33R protein in antibody-resistant spread. *J Gen Virol* **83**, 209–222.

Maa, J. S. & Esteban, M. (1987). Structural and functional studies of a 39,000-M_r immunodominant protein of vaccinia virus. *J Virol* **61**, 3910–3919.

Mackett, M., Smith, G. L. & Moss, B. (1985). The construction and characterization of vaccinia virus recombinants expressing foreign genes. In *DNA Cloning: a Practical Approach*, pp. 191–211. Edited by D. M. Glover. Oxford: IRL Press.

McDonald, D., Vodicka, M. A., Lucero, G., Svitkina, T. M., Borisy, G. G., Emerman, M. & Hope, T. J. (2002). Visualization of the intracellular behavior of HIV in living cells. *J Cell Biol* **159**, 441–452.

Mallardo, M., Schleich, S. & Krijnse Locker, J. (2001). Microtubule-dependent organization of vaccinia virus core-derived early mRNAs into distinct cytoplasmic structures. *Mol Biol Cell* **12**, 3875–3891.

Morgan, C. (1976). Vaccinia virus reexamined: development and release. *Virology* **73**, 43–58.

Moss, B. (2001). *Poxviridae*: the viruses and their replication. In *Fields Virology*, 4th edn, pp. 2849–2883. Edited by D. M. Knipe & P. M. Howley. Philadelphia: Lippincott Williams & WIlkins.

Parkinson, J. E. & Smith, G. L. (1994). Vaccinia virus gene A36R encodes a M_r 43–50 K protein on the surface of extracellular enveloped virus. *Virology* **204**, 376–390.

Pedersen, K., Snijder, E. J., Schleich, S., Roos, N., Griffiths, G. & Krijnse Locker, J. (2000). Characterization of vaccinia virus intracellular cores: implications for viral uncoating and core structure. *J Virol* **74**, 3525–3536.

Ploubidou, A., Moreau, V., Ashman, K., Reckmann, I., Gonzalez, C. & Way, M. (2000). Vaccinia virus infection disrupts microtubule organization and centrosome function. *EMBO J* **19**, 3932–3944.

Rietdorf, J., Ploubidou, A., Reckmann, I., Holmstrom, A., Frischknecht, F., Zettl, M., Zimmermann, T. & Way, M. (2001). Kinesin-dependent movement on microtubules precedes actin-based motility of vaccinia virus. *Nat Cell Biol* **3**, 992–1000.

Risco, C., Rodriguez, J. R., Lopez-Iglesias, C., Carrascosa, J. L., Esteban, M. & Rodriguez, D. (2002). Endoplasmic reticulum-Golgi intermediate compartment membranes and vimentin filaments participate in vaccinia virus assembly. *J Virol* **76**, 1839–1855.

Rodger, G. & Smith, G. L. (2002). Replacing the SCR domains of vaccinia virus protein B5R with EGFP causes a reduction in plaque size and actin tail formation but enveloped virions are still transported to the cell surface. *J Gen Virol* **83**, 323–332.

Rodriguez, J. F. & Smith, G. L. (1990). IPTG-dependent vaccinia virus: identification of a virus protein enabling virion envelopment by Golgi membrane and egress. *Nucleic Acids Res* **18**, 5347–5351.

Sanderson, C. M., Frischknecht, F., Way, M., Hollinshead, M. & Smith, G. L. (1998). Roles of vaccinia virus EEV-specific proteins in intracellular actin tail formation and low pH-induced cell–cell fusion. *J Gen Virol* **79**, 1415–1425.

Sanderson, C. M., Hollinshead, M. & Smith, G. L. (2000). The vaccinia virus A27L protein is needed for the microtubule-dependent transport of intracellular mature virus particles. *J Gen Virol* **81**, 47–58.

Smith, G. L., Vanderplasschen, A. & Law, M. (2002). The formation and function of extracellular enveloped vaccinia virus. *J Gen Virol* **83**, 2915–2931.

Sodeik, B. (2000). Mechanisms of viral transport in the cytoplasm. *Trends Microbiol* **8**, 465–472.

Sodeik, B., Doms, R. W., Ericsson, M., Hiller, G., Machamer, C. E., van't Hof, W., van Meer, G., Moss, B. & Griffiths, G. (1993). Assembly of vaccinia virus: role of the intermediate compartment between the endoplasmic reticulum and the Golgi stacks. *J Cell Biol* **121**, 521–541.

Sodeik, B., Ebersold, M. W. & Helenius, A. (1997). Microtubule-mediated transport of incoming herpes simplex virus 1 capsids to the nucleus. *J Cell Biol* **136**, 1007–1021.

Suomalainen, M., Nakano, M., Keller, S., Boucke, K., Stidwill, R. P. & Greber, U. F. (1999). Microtubule-dependent plus- and minus end-directed motilities are competing processes for nuclear targeting of adenovirus. *J Cell Biol* **144**, 657–672.

Towbin, H., Staehelin, T. & Gordon, J. (1979). Electrophoretic transfer of proteins from polyacrylamide gels to nitrocellulose sheets: procedure and some applications. *Proc Natl Acad Sci U S A* **76**, 4350–4354.

Vanderplasschen, A. & Smith, G. L. (1997). A novel virus binding assay using confocal microscopy: demonstration that the intracellular and extracellular vaccinia virions bind to different cellular receptors. *J Virol* **71**, 4032–4041.

Vanderplasschen, A., Hollinshead, M. & Smith, G. L. (1998). Intracellular and extracellular vaccinia virions enter cells by different mechanisms. *J Gen Virol* **79**, 877–887.

van Eijl, H., Hollinshead, M. & Smith, G. L. (2000). The vaccinia virus A36R protein is a type Ib membrane protein present on intracellular but not extracellular enveloped particles. *Virology* **271**, 26–36.

van Eijl, H., Hollinshead, M., Rodger, G., Zhang, W.-H. & Smith, G. L. (2002). The vaccinia virus F12L is associated with intracellular enveloped virus particles and is required for their egress to the cell surface. *J Gen Virol* **83**, 195–207.

Ward, B. M. & Moss, B. (2000). Golgi network targeting and plasma membrane internalization signals in vaccinia virus B5R envelope protein. *J Virol* **74**, 3771–3780.

Ward, B. M. & Moss, B. (2001a). Visualization of intracellular movement of vaccinia virus virions containing a green fluorescent protein-B5R membrane protein chimera. *J Virol* **75**, 4802–4813.

Ward, B. M. & Moss, B. (2001b). Vaccinia virus intracellular movement is associated with microtubules and independent of actin tails. *J Virol* **75**, 11651–11663.

Williams, O., Wolffe, E. J., Weisberg, A. S. & Merchlinsky, M. (1999). Vaccinia virus WR gene A5L is required for morphogenesis of mature virions. *J Virol* **73**, 4590–4599.

Wolffe, E. J., Weisberg, A. S. & Moss, B. (1998). Role for the vaccinia virus A36R outer envelope protein in the formation of virus-tipped actin-containing microvilli and cell-to-cell virus spread. *Virology* **244**, 20–26.

Zhang, W.-H., Wilcock, D. & Smith, G. L. (2000). The vaccinia virus F12L protein is required for actin tail formation, normal plaque size and virulence. *J Virol* **74**, 11663–11670.